NEW SHEAR ASSAY FOR THE SIMULTANEOUS DETERMINATION OF SHEAR STRENGTH AND SHEAR MODULUS IN SOLID WOOD: FINITE ELEMENT MODELING AND EXPERIMENTAL RESULTS

*Aleksandra Sretenovic**

Research Assistant

Ulrich Müller

Assistant Professor

Wolfgang Gindl†

Associate Professor

and

Alfred Teischinger

Professor
Institute of Wood Science and Technology
BOKU-University of Natural Resources and Applied Life Sciences
Gregor Mendel Strasse 33
A-1180 Vienna, Austria

(Received February 2003)

ABSTRACT

Using a new modified shear test set-up, the longitudinal shear strength and the shear modulus of solid wood were determined, and the resulting shear strength was compared to the widely used block shear test. The two studied wood species—Norway spruce and European larch—showed a clear increase of shear properties with increasing density. Regarding shear strength, the values determined with the ASTM D 143 block shear test were consistently, by a factor of 1.7, above those obtained with the new modified test set-up. Finite element analysis revealed the cause for this difference. At a load situation leading to a theoretical shear stress of 6 N/mm^2, obtained by dividing the applied load by the area of the shear plane, the distribution of shear stress in the ASTM block shear specimen is inhomogeneous. A high stress concentration near the loading edge (stress concentration factor = 2.3) is indicated, accompanied by low shear stress towards the opposite end of the shear plane. By contrast, shear stress is consistently high (5.8 N/mm^2) across the larger part of the new modified shear test specimen, leading to fracture at a lower applied external load than is the case for the ASTM block shear specimen. The distribution and intensity of shear stress in the new test set-up are fairly close to the stress state required for the determination of shear strength and shear modulus, and the new method therefore appears very suitable for the determination of the shear properties of solid wood.

Keywords: Density, European larch, finite element analysis, Norway spruce, shear strength, shear modulus, solid wood.

INTRODUCTION

Over many years, much effort and work have been expended to create a state of pure shearing stress to determine the shear strength and the shear modulus of wood. Several studies (Ylinen 1963; Askenazi 1976; Bodig and Jayne 1982; Liu 1984; Lang 1997) have dealt with the problem on how to induce shear stresses in a desired plane without a significant contribution of normal com-

* Corresponding author.
† Member of SWST.

pression, tension stresses, bending, or even torsional stresses. Although a pure state of shear stress cannot be achieved, two test methods prove most useful for determining shear properties. The losipescu shear test and the off-axis tensile test (Szalai 1992; Liu 2002) produce values presumably very close to the actual material properties, and these tests are therefore very useful. The new test method presented in this study presents a potential alternative to these methods, as neither strain gages nor complicated mathematical analysis are necessary. In addition, the new method allows the determination of the shear strength and the shear modulus in a single test. To assess the validity of the shear properties, a finite element analysis of the distribution of stresses within the specimen is performed. The resulting shear strength for spruce and larch wood is compared to the widely used block shear test, and the causes for the observed differences are explained on the basis of finite element analysis.

MATERIALS AND METHODS

Material preparation

Two shear test set-ups were considered: first the ASTM D 143 block-shear test (Fig. 1A) was studied for comparison, and second, a new set-up for solid wood (Fig. 1B) integrating elements of the ASTM D 1037 (1992) interlaminar and edgewise shear tests as well as the EN 789 (2002) interlaminar shear test that were originally designed for wood composites. The size of the block shear test specimens was scaled down to a cross section of 14 × 14 mm, instead of 50 × 50 mm to reduce the ultimate load to a maximum of 20 kN, but all proportions were kept as suggested by ASTM D 143. The tests specimens for the new test set-up were matched to a cross section of 14 × 14 mm and a length of 100 mm. Using phenol-formaldehyde glue, the test specimens were glued to beech support blocks of the same length measuring 25 × 25 mm in cross section. A phenolic resin with a shear strength of 17 N/mm^2 was used to avoid failure of the glueline. Beech was chosen because of its high G=1600 N/mm^2 and τ =20 N/mm^2 (Keylwerth 1951). The beech support blocks, in turn, were glued between two steel loading rails with a rapidly curing epoxy resin and additionally secured by 4 screws. (Fig. 1B).

Shear testing

Block shear tests were performed with 20 Norway spruce (*Picea abies*) and with 50 European larch (*Larix decidua*) samples with longitudinal grain orientation. One hundred spruce and 50 larch samples were tested using the new shear test set-up. All samples were conditioned to an equilibrium moisture content of 12 ± 1% before testing (see Table 1). The mechanical tests were performed on a Zwick/Roell Z100 kN universal testing machine, with a crosshead displacement rate of 0.6 mm/min. The block shear strength according to ASTM D 143 was computed by dividing the ultimate load by the area of the shear plane (i.e., 196 mm^2).

For the determination of shear strength with the new test set-up, the inclination of the sample was taken into account according to Eq. (1):

$$\tau = \frac{F_{max} \times \cos\alpha}{w \times 1} \quad (1)$$

where τ is the shear strength and F_{max} is the ultimate loading, the inclination of the sample α being 8°, and the area of the shear plane w × l (width × length) being 14 × 100 mm. The calculation of the shear strength performed by dividing the force by the area relies on the assumption that the entire external load is transformed into a shear stress that is homogeneously distributed across the whole shear plane. In this study, it will be shown that this is not the case and that different deviations from this ideal stress state are present in block shear specimens and the new shear specimens, respectively.

The longitudinal shear modulus is computed from the displacement of the crosshead of the testing machine using Eq. (2):

$$G = \frac{(F_1 - F_2) \times t}{w \times 1 \times \cos\alpha \times (u_1 - u_2)} \quad (2)$$

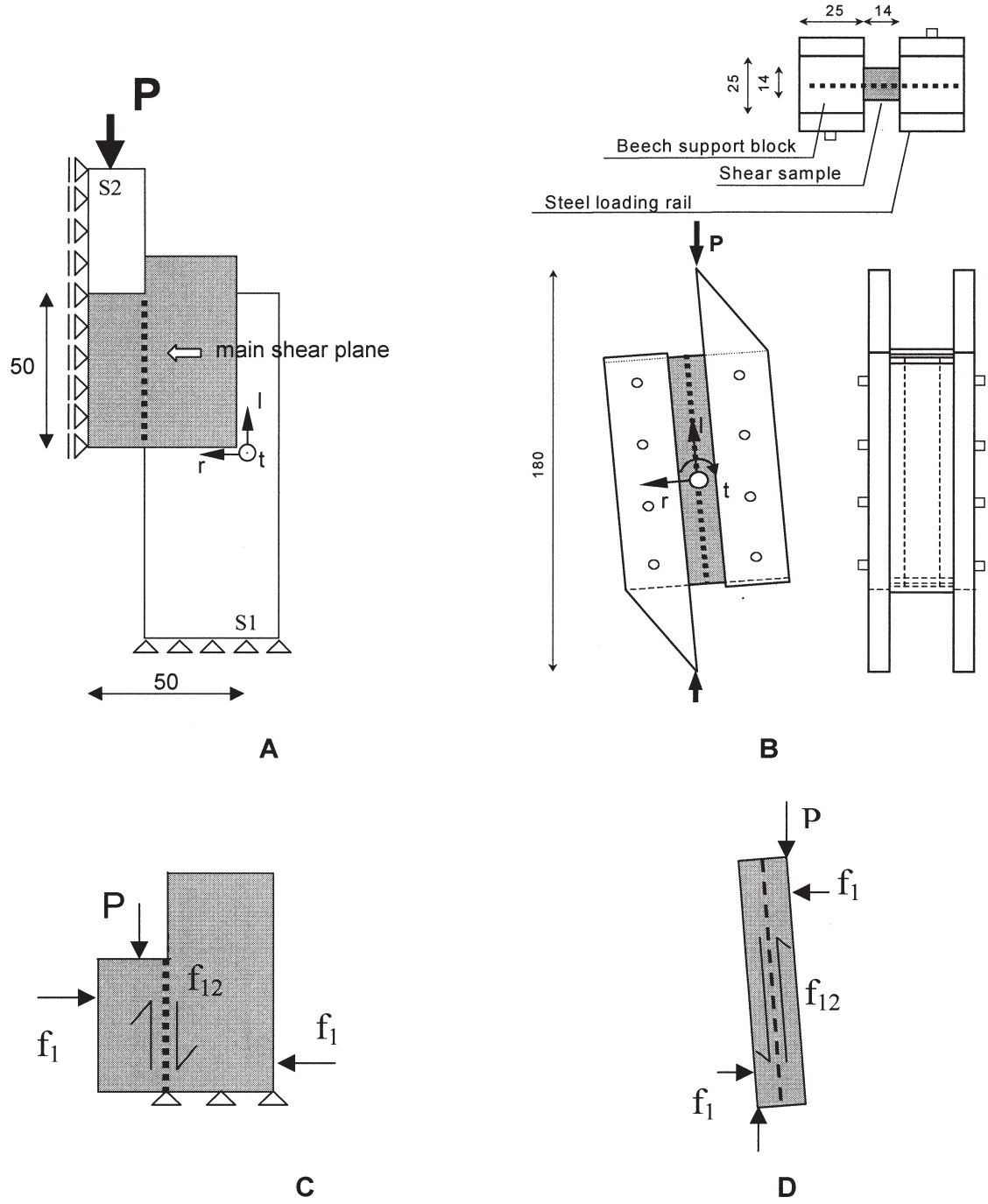

FIG. 1. (A) Scaled-down test set-up for block shear tests according to ASTM 143; (B) schematic of the new shear test set-up. Arrows mark the three orthogonal directions r = 1, I = 2, and t = 3; (C) Transformation of external load into shear and transverse stresses in block shear sample, and (D) in new shear sample.

TABLE 1. *Schedule of the mechanical tests, oven-dry density, and shear strength values.*

Wood species	Test method	Total number of samples	Density (g/cm^3)	Shear strength ± SD (N/mm^2)
Larch	new shear test	50	0.50	7.50 ± 1.54
	block shear test	50		13.74 ± 1.04
Spruce	new shear text	100	0.37	5.61 ± 1.35
	block shear test	20		9.42 ± 2.00

where F_1 is 10% of F_{max}, F_2 is 50% of F_{max}, u_1 is the deformation at F_1, u_2 is the deformation at F_2, and t is the sample thickness. To compute and eliminate the elastic deformations of the upper and lower fittings, the loading plates and the machine itself, a 25-mm-thick steel plate was clamped between the two pairs of steel loading rails instead of the wood sample before performing shear tests. The load-deformation data were recorded and subtracted from the load-deformation data of tested wood samples.

Finite element analysis

Depending on the test set-up chosen, shear testing yields different results for the ultimate shear strength. In order to determine which of the two set-ups was closer to ideal shear, a three-dimensional finite element analysis of stress distribution was performed. The numerical analysis was carried out by means of Abaqus software package, using CAE pre- and postprocessor. 3D model geometries were designed according to ASTM D 143 and the new shear test set-up. 3D modeling was preferred to earlier 2D modeling (Foschi and Barrett 1976), because a two-dimensional FE model overestimates stresses in one plane and neglects them in others, and it underestimates effects of compression and tension on shear stress distribution and the shear concentration factor. All dimensions were kept as in the experiments. The boundary conditions were chosen in a way that represented the experiment as closely as possible. In the ASTM D 143 block shear set-up, the steel base (S1) was restricted from displacements in each of the three degrees of freedom, whereas the loading plate (S2) was allowed to move only in the direction of loading, as is shown in Fig. 1A. In the case of the new test set-up, the loading rails were constrained for displacements in direction t, but the rotation in this direction was allowed (Fig. 1B). Contact between the steel blocks and the wood specimen perpendicular to the loading direction was defined using surface-to-surface contact elements with friction in the ASTM D 143 model; and in the case of new test set-up, all connections were made as tied constraints, since all parts were perfectly bonded together.

Ideal elastic material behavior was assumed for all parts in shear as well as for tension and compression. Table 2 gives the material characteristics used in the FE models taken from Kollmann and Côté (1968). Three-dimensional brick elements (linear hexahedral, element type C3D4) were used in Abaqus/CAE for both test set-ups, with the exception of the steel loading rails in the new test set-up, where element type C3D8 was chosen. A comparison between the results obtained from nonlinear and linear FE analyses resulted in a difference of about 3% for the ASTM D 143 model and 5% for the new shear test set-up. Therefore, linear FE-analysis was performed in both cases.

RESULTS

Figure 2 shows the shear strength determined according to ASTM D 143 as well as shear strength values obtained with the new test set-up plotted against density. Both data sets show an

TABLE 2. *Elastic constants used for the finite element models. Subscripts: 1 = radial, 2 = longitudinal, 3 = tangential.*

Material	E_1 (N/mm^2)	E_2 (N/mm^2)	E_3 (N/mm^2)	G_{12} (N/mm^2)	G_{13} (N/mm^2)	G_{23} (N/mm^2)	Nu_{12}	Nu_{13}	Nu_{23}
Spruce	650	14000	830	870	40	640	0.01	0.24	0.43
Beech	1200	17000	2300	1600	470	1100	0.04	0.45	0.45
Steel		210000						0.33	

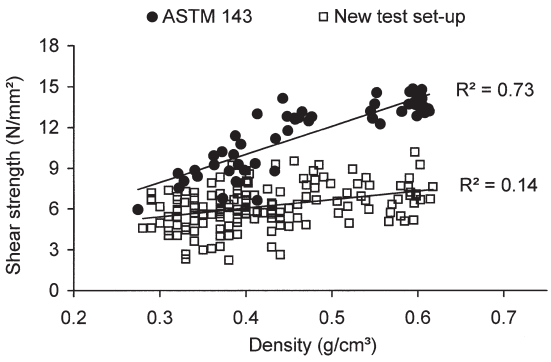

FIG. 2. Shear strength according to ASTM 143 and obtained with a new shear test set-up plotted against density in spruce and larch wood.

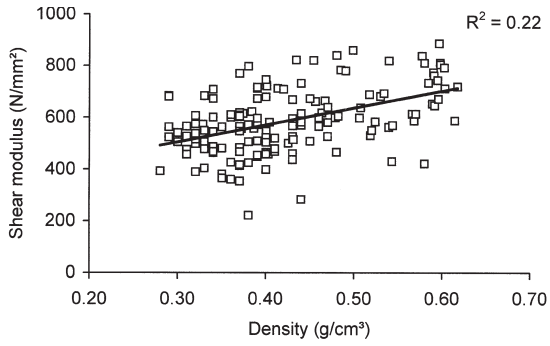

FIG. 4. Shear modulus obtained with the new shear test set-up plotted against density in spruce and larch wood.

increase of shear strength with increasing density. The shear strength values achieved with ASTM D 143 are consistently higher (mean value of 9.42 N/mm^2 for spruce and 13.74 N/mm^2 for larch, which corresponds to a factor 1.7) than the values measured by means of the new test set-up, which were mean values of 5.61 N/mm^2 for spruce and 7.50 N/mm^2 for larch, respectively (Table 1). The average oven-dry density of the shear specimens was 0.37 g/cm^3 for spruce and 0.50 g/cm^3 for larch, respectively (Table 1). No distinction was made between specimens sheared in the radial and tangential planes, respectively, because the shear strength of specimens tested in different modes did not differ significantly.

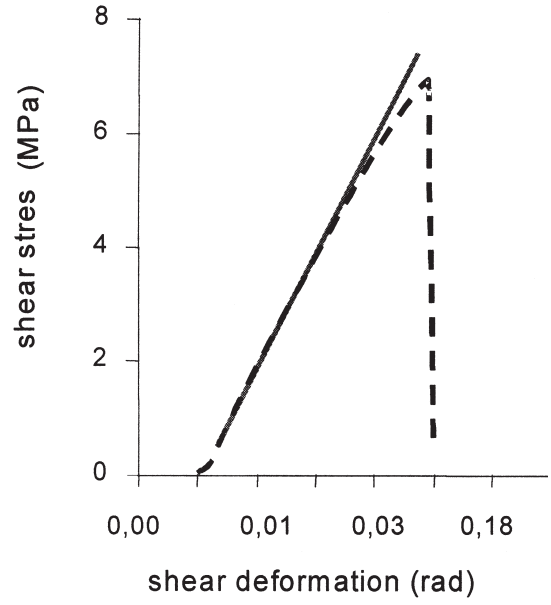

FIG. 3. Shear stress—deformation curve of larch normal wood.

Stress-deformation data were used to determine the shear modulus using the new test set-up as shown in Fig. 3. It can be seen that shear failure occurs rather abruptly, and plastic deformation of the specimen before fracture is very small. The resulting shear moduli are displayed in Fig. 4. The average shear modulus was 540 N/mm^2 for spruce and 663 N/mm^2 for larch, respectively. A highly significant linear increase of the shear modulus with increasing density was observed in spruce and larch normal wood for both samples (Fig. 4).

The distribution of shear stress over the specimen surface calculated by FE-analysis is plotted in Fig. 5. Shear stress is inhomogeneously distributed in the ASTM specimen as compared to the new test set-up. Line plots of shear stress (Fig. 6) over the plane of fracture indicated by dotted lines in Fig. 1, illustrate this fact more clearly. According to the load step chosen in the numerical model, the shear stress in the specimen should be 6 N/mm^2, as obtained by dividing the loading force by the area of the shear plane. Figure 6 shows that at a load corresponding to a shear stress of 6 N/mm^2, the actual stress is far below

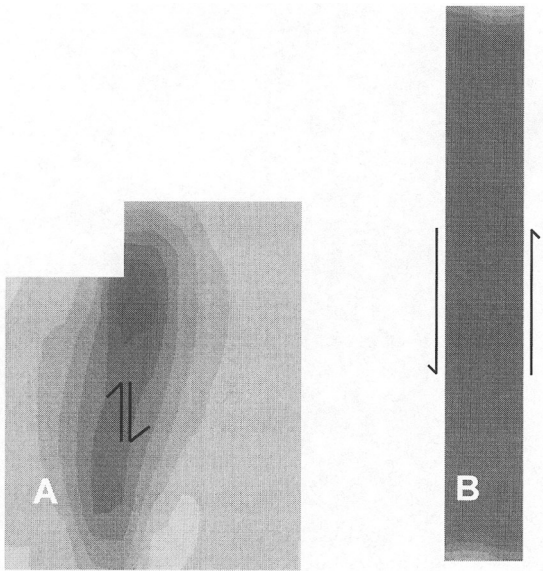

FIG. 5. Shear stress distribution in block ASTM test set-up (A), and new modified test set-up (B). Zones of high shear stress are darker than zones of low shear stress.

this level in most of the ASTM specimen. In this specimen, the shear stress is high (5 N/mm^2) at the loading corner and decreases towards the opposite end of the shear plane The stress concentration factor at the loading edge of the ASTM specimen calculated by dividing the maximum stress by the average stress level is 2.32.

Regarding the new test set-up, Fig. 5 and Fig. 6 show a much more homogeneous stress distribution compared to the ASTM specimen. In the larger part of the new specimen, the shear stress, with 5.8 N/mm^2, is very close to the theoretical value of 6 N/mm^2 expected due to the chosen load step settings. At both ends of the new specimen, the shear stress decreases to 3.6 N/mm^2.

For the determination of the shear modulus, the amount of deformation taking place in other parts of the new specimen, apart from the spruce part, is of interest. Since the deformation of the steel loading rails is part of the machine compliance determined prior to testing and thus compensated before the modulus was calculated, the deformation of the beech parts was of interest. Figure 7 shows the distribution of shear stress across the beech blocks and the spruce specimen (the path is indicated by a dotted line in Fig. 1). It can be seen that only a very small part of the beech blocks is affected by shear stress. Figure 8 depicts the distribution of transverse stress over the specimen surface. The compression transverse stresses normal to the shearing plane of the block shear model is small but significant and, concerning the new shear test set-up, transverse tensile and compression stresses are present only on the top and bottom very close to the edges.

DISCUSSION

The results presented above clearly demonstrate the advantages of the new shear test set-up compared to block shear tests, as proven by finite element analysis, i.e., homogeneous stress distribution in the larger part of the new shear

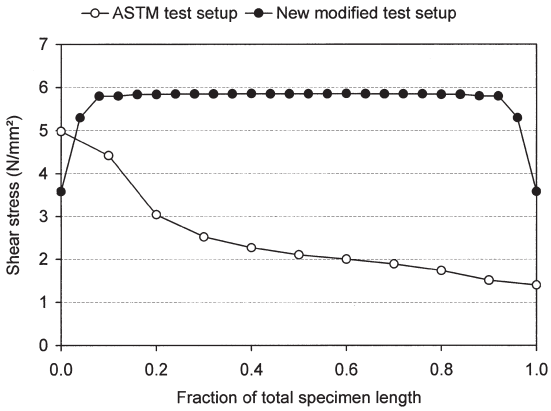

FIG. 6. Shear stress distribution along the spruce specimens obtained from FE-analysis.

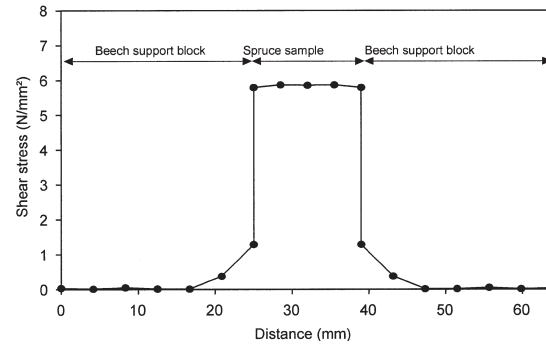

FIG. 7. Shear stress distribution in spruce sample and two beech support blocks of the new shear test set-up obtained in FE-modelling.

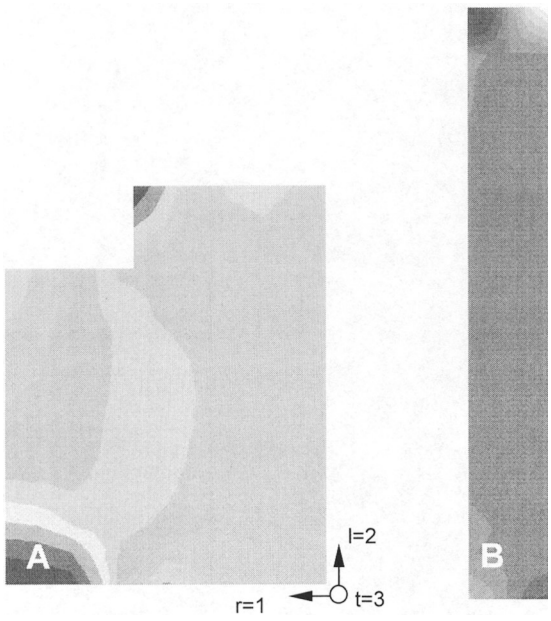

FIG. 8. Transverse stress distribution in the block ASTM test set-up (A), and the new modified test set-up (B). Zones of tensile transverse stress are dark and zones of compressive transverse stress are bright.

specimen, lower transverse stresses perpendicular to the shear plane, direct determination of shear strength and shear modulus and lower external load necessary to create failure in new test set-up. As depicted in Fig. 3, shear failure occurs abruptly, the amount of plastic deformation being very small. It is thus justified to analyze the shear stress distribution assuming linear elastic material behavior.

Block shear tests, as described in ASTM D 143 (1992) or in DIN 52187 (1979) suffer from substantial disadvantages, but are, nonetheless, widely used. First, a stress concentration occurs at the loading corner of the specimen (Figs. 5 and 6). Second, disturbing stresses perpendicular to the shear plane develop during shear testing, and their influence is much higher than in the new test method. Third, the shear stress in the block shear sample is inhomogeneously distributed along the main shear plane. The stress concentration factor calculated for the ASTM D 143 specimen subjected to finite element analysis is 2.32, which agrees well with published values of at least 2 (Coker and Coleman 1935; Radcliffe and Suddarth 1955), and up to 2.36, respectively (Cramer et al. 1984; Soltis and Rammer 1994). Radcliffe and Suddarth (1955) applied strain gages to wood specimens to show that the stress distribution was in fact unsymmetrical. Soltis and Rammer (1994) performed a regression analysis on shear area and shear strength to show that beam shear strength is related to shear block strength.

In addition to the inhomogeneous distribution of shear stress revealed in Figs. 5 and 6, block shear specimens are also subjected to substantial transverse compression stress normal to the shear plane (Fig. 8), which affect shear behavior. Figures 1C and 1D schematically describe how the external load is transformed into a shear stress and transverse stress normal to the shear plane in the ASTM sample and in the new sample. Equation (3) is derived from the theory of distortion (Norris 1962),

$$\frac{f_1^2}{F_1^2} + \frac{f_{12}^2}{F_{12}^2} = 1 \qquad (3)$$

where f_1 is stress normal to the shear plane, f_{12} is shear stress, and F_1 and F_{12} are the critical transverse and shear stress, respectively, for the material, states that shear stress decreases when transverse stress increases. Transverse stresses perpendicular to the shear plane are therefore the reason for the relatively low average level of shear stress observed in the block shear specimen at a given load, as compared to the new test set-up. A higher level of external load is thus necessary to create the shear stress necessary for failure in a block shear specimen, which is affected by substantial transverse compression stresses normal to the shear plane. In comparison, the external load necessary to create failure in the new test set-up, which shows only very small transverse stresses, is lower, as is reflected by the experimental results displayed in Fig. 2. The theoretical considerations described in Eq. (3) agree well with results examining the relationship between compressive load perpendicular to the grain and shear strength of wood parallel to the grain published by Mandery

(1968), although he doubted the validity of Eq. (3) for wood. Mandery (1968) found that shear strength increased proportionally with increasing external compression load normal to the shear plane.

Because of the differences in the distribution and level of internal shear stress described above, the shear strength determined with the new test set-up is significantly lower than published average values of 6.7 N/mm^2 for spruce and 9.7 N/mm^2 for larch, respectively, based on block shear tests (Sell 1989; Niemz 1993, Forest Products Laboratory 1999). Similarly, Liu (1984) also observed significantly lower shear strength values for Douglas-fir tested with an optimized test geometry with minimized stress normal to the shear plane occurrence, compared to ASTM D 143.

The shear moduli for spruce (540 N/mm^2) and larch (663 N/mm^2) determined with the new test set-up are, again, rather low compared to shear moduli for different softwood species ranging from 650 to 910 N/mm^2 (Keylwerth 1951; Zhang and Sliker 1991; Divos et al. 1998; Liu 2000). The relatively low shear moduli measured with the new test set-up are due to the deformation of the beech supporting blocks, which was not considered in the calculation. When the shear stress plotted against the position in the test set-up in Fig. 7 is divided by G of the respective wood species, the distribution of shear strain across the sample thickness is obtained. The area under the graph, which can be obtained by numerical integration, is equivalent to the total shear deformation. Assuming a G of 1600 N/mm^2 for beech, the total deformation arising from shear in the two beech blocks is 0.00083 radians per N/mm^2 shear stress. When this deformation is subtracted from u_1 and u_2 in Eq. (2), values of G 6% higher than without correction for deformation in the beech supports are obtained. The fact that a small amount of deformation occurs also in the beech supports, which leads to an underestimation of G, is a disadvantage of the new test set-up.

Previous investigations and analyses demonstrated the complexity of stress phenomena in a standard block shear test specimen. Experimental results in a combination with three-dimensional finite element analyses were able to confirm the effects of stress concentrations at the notch of the ASTM model and the effect of transverse compression stresses perpendicular to grain (transverse to the shear plane). Concerning the new shear test set-up, it could be demonstrated that it provides a good means for the direct determination of shear strength and shear modulus, which showed a linear relationship with density. Taking into account the natural variability of wood, it is proposed that resulting shear strength is close to actual material properties. Regarding G, a correction for deformation taking place in the beech support blocks is necessary.

ACKNOWLEDGMENT

Financial support by the Austrian Science Fund (FWF), Project P15410-B03, is gratefully acknowledged.

REFERENCES

American Society of Testing and Materials (ASTM). 1992. Standard methods of testing small clear specimens of timber. ASTM D-143-83. Test methods of evaluating the properties of wood-base fiber and particle panel materials. ASTM D-1037-91. Vol. 04.09. Wood. ASTM, West Conshokocken, PA.

Askenazi, A. K. 1976. Anisotropy of wood and wood-base materials. 1st ed. Izdatelstvo Lesnaja Promuslennosty, Moscow, USSR (in Russian).

Bodig, J., and B. A. Jayne. 1982. Mechanics of wood and wood composites. Van Nostrand Reinhold Co., New York, NY. P. 712.

Coker, E. G., and G. P. Coleman. 1935. Photo-elastic investigation of shear tests of timber. Selected Engineering Pap. No. 174, The Institution of Civil Engineers, London, England.

Cramer, S. M., J. R. Goodman, J. Bodig, and F. W. Smith. 1984. Failure modeling of wood structural members. Structural Res. No. 51, Civil Engineering Dept., Colorado State Univ., Fort Collins, CO.

Din 52187. 1979. Testing of wood: Determination of ultimate shearing stress parallel to grain. Normenausschuß Holz im DIN.

Divos, F., T. Tanaka, H. Nagao, and H. Kato. 1998. Determination of shear modulus on construction size timber. Wood Sci. Technol. 32:393–402.

En 789. 2002. Timber structures—Test methods—Determination of mechanical properties of wood-based panels. Fachnormenausschuß 012 Holzbau.

FOREST PRODUCTS LABORATORY. 1999. Wood Handbook—Wood as an Engineering Material. USDA Forest Serv. Forest Prod. Lab., Madison, WI.

FOSCHI, R. O., AND J. D. BARRETT. 1976. Longitudinal shear strength of Douglas-fir. Can. J. Civil Eng. 3(2): 198–208.

HIBBIT, KARLSSON & SORENSEN, INC. 2001. ABAQUS/CAE and Standard-User's Manual.

KEYLWERTH, R. 1951. Die anisotrope Elastizität des Holzes und der Lagehölzer. Deutscher Ingenieur-Verlage GmbH, Düsseldorf.

KOLLMANN, F. P., AND W. A. CÔTÉ. 1968. Principles of wood science and technology, Springer-Verlag-Berlin, Heidelberg, New York.

LANG, E. M. 1997. An alternative method for shear strength assessment. Forest Prod. Soc. Vol. 47, No. 11/12.

LIU, J. Y. 1984. New shear strength test for solid wood. Wood Fiber Sci. 8(4):252–261.

———. 2000. Effects of shear coupling on shear properties of wood. Wood Fiber Sci. 32(4):458–465.

———. 2002. Analysis of off-axis tension of wood specimens. Wood Fiber Sci. 34:205–211.

MANDERY, W. L. 1968. Relationship between perpendicular compressive stress and shear strength of wood, Wood Sci. 1:(3).

MÜLLER, U., A. SRETENOVIC, W. GINDL, M. GRABNER, R. WIMMER, AND A. TEISCHINGER. 2003. Effects of macro- and micro-structural variability on the shear behaviour of softwood. Submitted.

NIEMZ, P. 1993. Physik des Holzes und der Holzwerkstoffe. DRW-Verlag, Leinfelden-Echterdingen.

NORRIS, C. B. 1962. Strength of orthotropic materials subjected to combined stresses. USDA For. Prod. Lab. Rept. 1816. Madison, WI.

RADCLIFFE, B. M., AND S. K. SUDARTH. 1955. The notched beam shear test for wood. Forest Prod. J. 5(2):131–135.

SELL, J. 1989. Eigenschaften und Kenngrößen von Holzarten. by LIGNUM, Schweizerische Arbeitsgemeinschft für das Holz, Zürich.

SOLTIS, L. A., AND D. R. RAMMER. 1994. Shear strength of unchecked glue-laminated beams. Forest Prod. J. 44(1): 51–57.

SZALAI, J. 1992. Indirekte Bestimmung der Scherfestigkeit des Holzes mit Hilfe der anisotropen Festigkeitstheorie. Holz Roh-Werk. 50:233–238.

YLINEN, A. 1963. A comparative study of different types of shear tests of wood. Paper presented at the Fifth Conference of Wood Technology. USDA Forest Serv., Forest Prod. Lab., Madison, WI.

ZHANG, W., AND A. SLIKER. 1991. Measuring shear moduli in wood with small tension and compression samples. Wood Fiber Sci. 23(1):58–68.